Journal of Computer-Aided Molecular Design, **13:** 233–242, 1999.
KLUWER/ESCOM
© 1999 *Kluwer Academic Publishers. Printed in the Netherlands.*

Comparison of azacyclic urea A-98881 as HIV-1 protease inhibitor with cage dimeric *N*-benzyl 4-(4-methoxyphenyl)-1,4-dihydropyridine as representative of a novel class of HIV-1 protease inhibitors: A molecular modeling study

Andreas Hilgeroth[a,*], Romy Fleischer[a], Michael Wiese[a] & Frank W. Heinemann[b]
[a]*Institute for Pharmaceutical Chemistry, Department of Pharmacy, Martin-Luther-University Halle-Wittenberg, Wolfgang-Langenbeck-Strasse 4, D-06120 Halle, Germany;* [b]*Institute for Inorganic Chemistry II, Friedrich-Alexander-University Erlangen-Nürnberg, Egerlandstrasse 1, D-91058 Erlangen, Germany*

Received 19 June 1998; Accepted 27 October 1998

Key words: centrosymmetry, CoMFA-Field fit, GRID, HIV-1 protease, X-ray crystal structure

Summary

The functional groups of cage dimeric *N*-alkyl substituted 3,5-bis(hydroxymethyl)-4-(4-methoxyphenyl)-1,4-dihydropyridines are similar to those of cyclic and azacyclic ureas that are potent inhibitors of HIV-1 protease of the dihydroxyethylene- and hydroxyethylene type, respectively. In the following study the conformity of common functional groups is investigated concerning their orientation in space as well as in the enzyme HIV-1 protease. Starting from X-ray crystal data of the centrosymmetric cage dimeric *N*-benzyl derivative with ester groups, the derivative with hydroxymethylene groups was built and a systematic conformational search was performed for the conformationally important torsion angles considering electrostatic and van der Waals interactions. From the huge number of conformations those comprising centrosymmetrical and C_2-symmetrical energy minima were selected and minimized. The three remaining conformers were fitted to the azacyclic urea A-98881 selected from the HIV-1 protease enzyme-inhibitor complex using the centroids of the corresponding aromatic residues and additionally by the field fit option of the Advanced CoMFA module of SYBYL. Interestingly, the energetically most favourable one, which, additionally, possesses C_2-symmetry like the active site cavity of HIV-1 protease, showed the best fit. Comparing the electrostatic potential (EP) of the latter with the EP of A-98881 the aromatic residues show excellent accordance. Slight differences in the extent of the EP were found in the areas of the hydroxymethylene groups of the cage dimer and the single hydroxy group as well as the urea carbonyl group of A-98881, respectively. In order to compare the binding possibilities to the enzyme HIV-1 protease for the cage dimer and A-98881, their interaction fields with certain probes (CH_3 for alkyl, NHamide, and carbonyl, O^- of COO^-), representing the decisive functional groups of the active site, have been calculated using GRID and projected into the enzyme placing the structures according to the position of A-98881 in the enzyme-inhibitor complex. The strongest calculated fields of the O^- probe were found near Asp 25 for both structures. Another respective conformity consists in the overlap of the fields for the NHamide probe near Ile 50 and 50′ for the investigated cage dimer and A-98881.

Introduction

Since the discovery of the human immunodeficiency virus type-1 (HIV-1) as causative agent of acquired immunodeficiency syndrome (AIDS) [1] several nucleoside analogues like zidovudine (AZT), didanosine (ddI) or zalcitabine (ddC) as inhibitors of the reverse transcriptase (RT) have been developed. They remained the exclusive therapeutics of the HIV infection until the discovery of the HIV-1 protease (PR)

*To whom correspondence should be addressed. E-mail: hilgeroth@pharmazie.uni-halle.de.

offered a novel target enzyme for the development of highly potent protease inhibitors [2,3]. As a homodimer of the aspartyl protease family PR consists of two identical subunits with 99 amino acids, respectively, unlike any other aspartyl protease [2]. The resolution of PR by X-ray crystal structure analysis proved the active site cavity to have a C_2-symmetry with the two Asp residues 25 and 25′ at the active cleavage site [4]. A *gag*-PR-(*pol*) precursor is converted into the active PR by autocatalysis [2]. PR cleaves *gag-pol* protein precursor in active enzymes (RT, ribonuclease and integrase) and *gag* protein precursors in matrix, capsid and nucleocapsid which form the intact virus capsid. The inhibition of PR firstly reported for pepstatin A [5] leads to unmatured virus particles which themselves are non-infectious [2]. Meanwhile a number of potent peptidomimetic HIV-1 protease inhibitors (PI) has been developed. They contain transition-state inserts in place of the dipeptidic cleavage site of the substrates [3,6]. Due to their peptide analogue structures the oral bioavailability is poor. The necessary high therapeutic doses cause extensive side effects [3]. Furthermore, resistances arise, so that the development of novel substances with reduced or non-peptidic structures is required. C_2-symmetric cyclic and non-symmetric azacyclic ureas represent one promising class of such non-peptidic PI of the dihydroxy- and hydroxyethylene type, respectively [7,8]. In contrast to previous PI they displace water 301 in the enzyme active site cavity by direct binding of their carbonyl urea group to Ile 50 and 50′ [7,8]. We synthesized cage dimeric *N*-alkyl substituted 3,5-bis(hydroxymethyl)-4-aryl-1,4-dihydropyridines as novel PR inhibitors and anti-HIV agents, respectively [9,10]. As being centrosymmetric molecules, which possess a C_2-axis in their molecular structure as well, their high symmetry promises them as interesting structures for a potentially symmetrical binding to PR. In the following study we investigate conformities in the location of common functional groups of a cage dimeric *N*-benzyl-1,4-dihydropyridine and the azacyclic urea A-98881 as bound in the enzyme-inhibitor complex. The derived molecular properties, i.e. the electrostatic potential (EP) and the interaction fields calculated with GRID are compared.

Materials and methods

X-ray diffraction analysis of cage dimeric *N*-benzyl-3,5-diethoxycarbonyl-4-(4-methoxyphenyl)-1,4-dihydropyridine **1** [10]: A colourless prism shaped crystal $C_{50}H_{54}N_2O_{10}$ (from ethanol), crystal size $0.3 \times 0.2 \times 0.2$ mm^3, was measured at room temperature by using a Nicolet R3m/V Diffractometer with Mo-K_α radiation ($\lambda = 0.71073$ Å) and a graphite monochromator. A total of 4308 reflections were collected in ω scanning mode in the range of $4.16° \leq 2\Theta \leq 50.1°$; h, k, l range from -9, -13, -15 to 1, 13, 15. Crystal system: Triclinic, space group $P\bar{1}$, $Z = 1$, $a = 8.128(3)$ Å, $b = 11.234(6)$ Å, $c = 13.224(4)$ Å, $\alpha = 69.78(3)°$, $\beta = 86.09(3)°$, $\gamma = 81.77(4)°$; $V = 1121.2(8)$ Å^3; $D_x = 1.248$ g cm^{-3}; $\mu = 0.087$ mm^{-1}. The structure was solved by direct methods (SHELXTL 5.03 [11]) using 3958 independent reflections. Structure refinement: Full-matrix least squares methods on F^2 using SHELXTL 5.03 [11], all the non-hydrogen atoms with anisotropic displacement parameters. Hydrogen positions were taken from a difference Fourier synthesis and fixed on their positions with a common isotropic thermal parameter during the structure refinement. The refinement converged to a final $wR^2 = 0.0949$ for 4308 unique reflections and $R^1 = 0.0443$ for 1144 observed reflections [$I_0 > 2.0\sigma(I_0)$] and 280 refined parameters.

Molecular modeling investigations were performed with SYBYL 6.4 [12] running on a Silicon Graphics R4000 workstation. The Gasteiger-Hückel and semiempirical AM1 method as implemented in SYBYL were used to calculate partial charges of the molecules [13,14] and a distance-dependent dielectric constant was used.

As the dimer **2** derived from the X-ray crystal structure of **1** (Figure 1) with ester groups replaced by hydroxymethylene groups possesses 10 torsion angles that must be considered, the systematic conformational search was performed for each half of the dimer. The conformationally important torsion angles (RB1, RB2 and RB3, Figure 2) were varied in 10° steps. To avoid the loss of energetically feasible conformations the default settings of the van der Waals factors were reduced by 0.1 and also RB4 and RB5 were rotated in 30° steps. From the result of the search local energy minima were selected in two steps with a locally written version of the FAMILY algorithm [15,16]. The algorithm searches for local energy minima in a torsion angle space. A conformation is considered to be a local energy minimum if all conformations that differ by one rotational step size possess higher energy. As the algorithm implemented in SYBYL is tediously slow if applied to a large number of conformations a program was written to perform this task. It allows

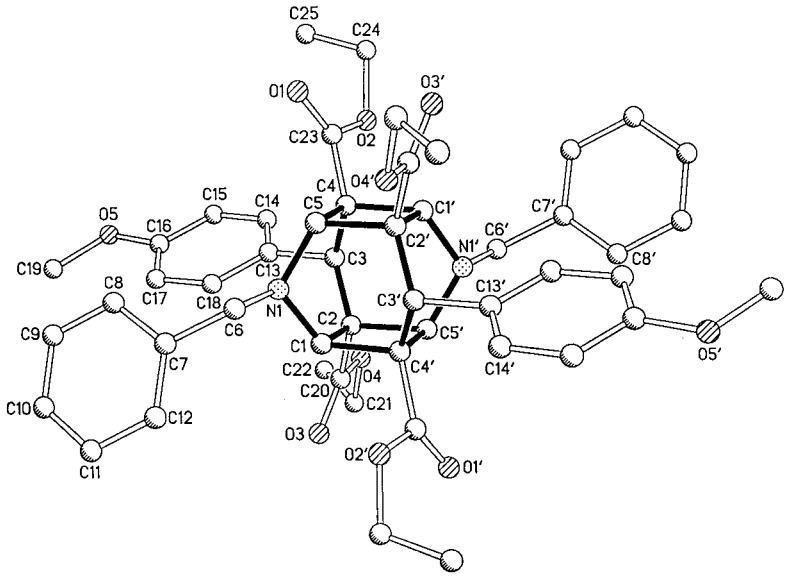

Figure 1. Molecular structure of 3,9-dibenzyl-1,5,7,11-tetraethoxycarbonyl-6,12-bis(4-methoxyphenyl)-3,9-diazahexacyclo[6.4.0.0^{2,7}.0^{4,11}.0^{5,10}] dodecane (**1**).

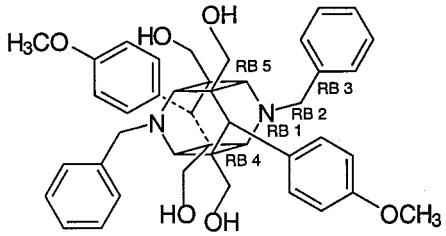

2

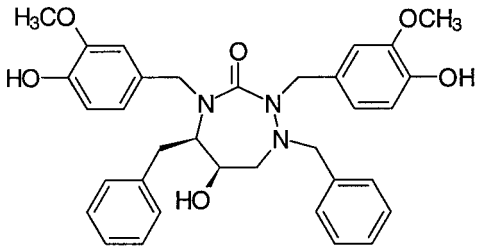

A-98881

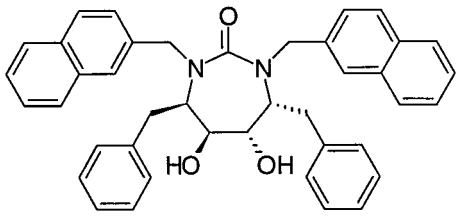

3

Figure 2. Chemical structures of 3,9-dibenzyl-1,5,7,11-tetra(hydroxymethyl)-6,12-bis(4-methoxyphenyl)-3,9-diazahexacyclo[6.4.0.0^{2,7}.0^{4,11}.0^{5,10}] dodecane (**2**) with rotational bond (RB) numbering, A-98881 and cyclic urea **3** [7].

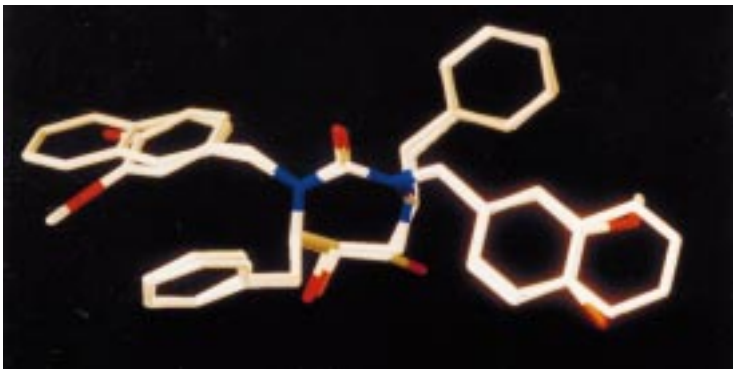

Figure 3. A-98881 and cyclic urea **3** as bound in the active site cavity of HIV-1 protease.

additionally to 'ignore' torsion angles that are not considered to be conformationally important, but have to be rotated in order to avoid loss of energetically feasible conformations due to steric hindrance (e.g. RB4 and 5). For each tuple of torsion angles considered to be relevant (RB1, RB2 and RB3) the energetically lowest conformation of the 'ignored' torsion angles that correspond to the two hydroxymethylene chains was selected. In the second step, conformations comprising local energy minima in the reduced search space of the three important torsion angles were selected yielding 4 local energy minima conformations. In this way the occurrence of local minima differing only in the torsion angles of the hydroxymethylene chains was avoided.

For each of these four conformations a systematic search of the other half of the dimer was performed in an identical way leading to between 5 and 7 local minima. The symmetrical conformations were selected and extensively energy minimized with the Tripos force field [17] (force field engine with a 0.001 kcal mol^{-1} $Å^{-1}$ energy gradient convergence criterion, distance dependent electrostatics) as well as with AM1. During minimization several structures converged to the same minimum. The three minimized conformations that possessed nearly centrosymmetry or C_2-symmetry, respectively, with deviations of less than 5° were selected for further studies.

Molecular dynamics simulations were carried out with a time step of 0.001 ps in vacuo and in DMSO. The system was heated up in 1 ps to 300 K or 370 K, respectively, and then equilibrated for 30 ps, and a constant-temperature dynamics simulation was then performed for 100 ps. The trajectory was recorded every 0.1 ps. The charges and starting geometry of DMSO used as solvent were calculated by AM1.

The calculation of the interaction fields was done with the program GRID V15 [18]. The default parameters of the different probes were used, the grid spacing was 1 Å and the grid extended the molecules by 5 Å in each direction. The same grid setting was used for all probes.

^{1}H-NMR spectra were recorded on a Varian Gemini 500 at 500 MHz with tetramethylsilane as internal standard in d_6-DMSO at room temperature.

Results and discussion

Energy minimization of the conformations obtained from the systematic search with the Tripos force field led to two C_2-symmetric (**2a**, **b**) and one centrosymmetric (**2c**) conformations. If the starting structures were minimized by AM1 one C_2-symmetric [**2a(AM1)**], a centrosymmetric [**2c(AM1)**] and one non-symmetric conformation [**2b(AM1)**] with a loss of symmetry for one half of the molecule were obtained. The energetically most favourable conformations **2a** and **2a(AM1)** were geometrically nearly identical concerning the methoxyphenyl residues and showed only slight deviation for the benzylic groups. The geometries of the less favourable **2c** and **2c (AM1)** conformations were also identical (Table 3). Moreover, a comparison with the precursor X-ray structure of **1** was performed. For **2a** the location and orientation of one half of the molecule showed a good conformity with the X-ray structure, while the other half deviated in the torsion angles due to the change from centro- to C_2-symmetry. Conformation **2b** showed larger deviations in the torsion angles from the X-ray structure, however the location of the centers of the aromatic rings were comparable. For the least stable conformation **2c** the largest deviation from the X-ray

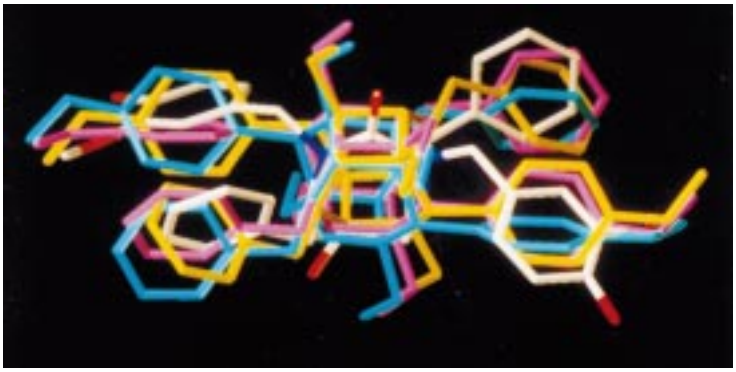

Figure 4. Conformers **2a** (magenta), **2b** (cyan) and **2c** (yellow) fitted to A-98881 after CoMFA field fit.

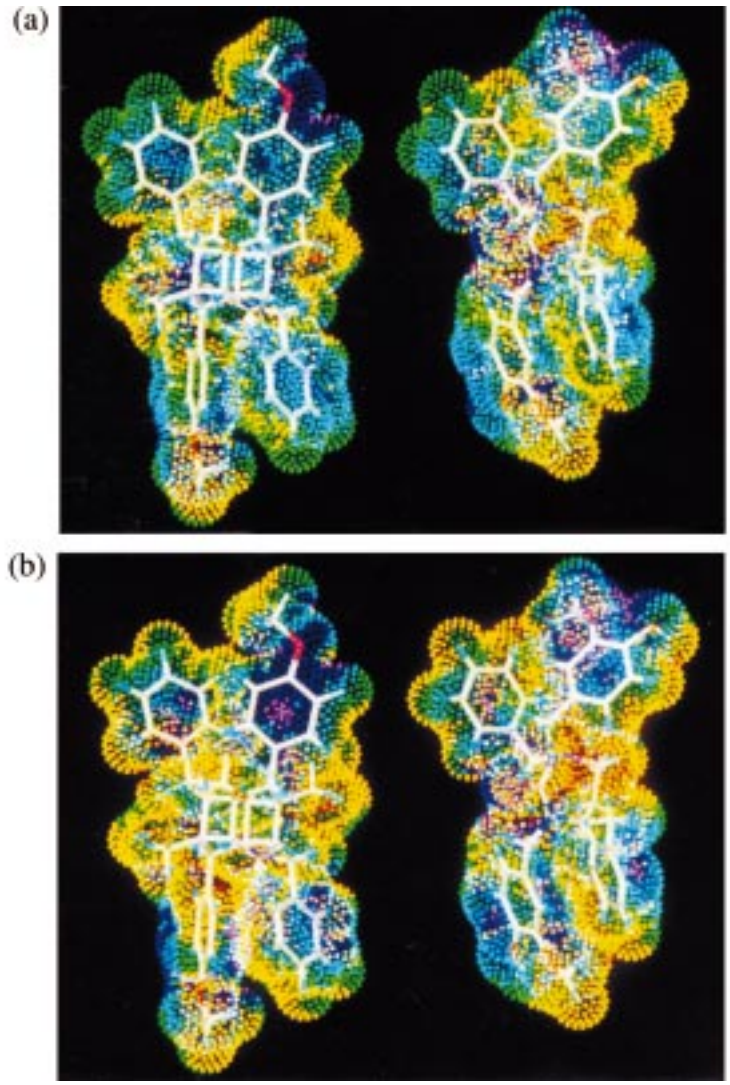

Figure 5. Electrostatic potentials of conformer **2a** (left) and A-98881 (right) displayed on the van der Waals surface. (a) Gasteiger-Hückel charges; (b) AM1 derived charges. The following color coding was used: above 25 kcal/mol (red), 10 to 25 (orange), 3.3 to 10 (yellow), 0.0 to 3.3 (green), −3.3 to 0.0 (cyan), −10 to −3.3 (blue), −25 to −10 (purple) and below −25 (white).

Table 1. Atomic coordinates ($\times 10^4$) and equivalent isotropic displacement parameters ($pm^2 \times 10^{-1}$), U_{eq} (Å $\times 10^3$)

	x	y	z	U_{eq}[a]
N(1)	−1003(3)	−1093(3)	4447(2)	38(1)
O(1)	−4520(3)	1838(2)	4390(2)	72(1)
O(2)	−2742(3)	3305(2)	4008(2)	53(1)
O(3)	3424(3)	−386(3)	2850(2)	73(1)
O(4)	2863(3)	1712(2)	2577(2)	55(1)
O(5)	−2627(3)	2636(3)	−711(2)	70(1)
C(1)	783(4)	−1030(3)	4399(3)	39(1)
C(2)	1213(4)	368(3)	3889(3)	35(1)
C(3)	−259(4)	1436(3)	3544(3)	35(1)
C(4)	−1563(4)	1149(3)	4468(3)	35(1)
C(5)	−1945(4)	−274(3)	4978(3)	40(1)
C(6)	−1453(4)	−2410(3)	4743(3)	46(1)
C(7)	−1368(5)	−2826(3)	3753(3)	41(1)
C(8)	−2571(5)	−2269(4)	2977(4)	63(1)
C(9)	−2444(6)	−2614(5)	2033(4)	83(2)
C(10)	−1172(7)	−3501(5)	1921(4)	83(2)
C811)	−21(6)	−4059(4)	2686(4)	74(1)
C(12)	−95(5)	−3699(4)	3617(3)	54(1)
C(13)	−904(4)	1674(4)	2422(3)	40(1)
C(14)	−1312(5)	2930(4)	1744(3)	51(1)
C(15)	−1877(5)	3231(4)	709(3)	58(1)
C(16)	−2002(5)	2242(4)	325(3)	53(1)
C(17)	−1572(5)	985(4)	957(3)	53(1)
C(18)	−1013(4)	701(3)	2012(3)	48(1)
C(19)	−2627(6)	1664(4)	−1180(3)	84(2)
C(20)	2615(5)	479(4)	3053(3)	45(1)
C(21)	4172(5)	1975(4)	1748(4)	76(2)
C(22)	3500(6)	3001(7)	811(4)	192(4)
C(23)	−3119(5)	2095(4)	4266(3)	44(1)
C(24)	−4147(6)	4311(4)	3955(4)	75(1)
C(25)	−5075(6)	4695(4)	2955(4)	100(2)
H(1)	1345	−1497	4009	80
H(3)	111	2244	3499	80
H(5)	−3240	−410	5022	80
H(6A)	−2583	−2372	5055	80
H(6B)	−653	−3063	5378	80
H(8)	−3618	−1519	3054	80
H(9)	−3393	2024	1498	80
H(10)	−1226	−3676	1231	80
H(11)	884	−4765	2754	80
H(12)	709	−4085	4094	80
H(14)	−1324	3602	1986	80
H(15)	−2230	4178	194	80
H(17)	−1639	219	741	80
H(18)	−685	−377	−2511	80
H(19A)	−3082	2067	−1856	80
H(19B)	−1330	1044	−1151	80
H(19C)	−3432	942	−721	80
H(21A)	4319	1308	1224	80
H(21B)	5349	1594	2087	80
H(22A)	3223	1916	674	80
H(22B)	4509	3200	262	80
H(22C)	2669	3397	634	80
H(24A)	−3682	5015	4003	80
H(24B)	−4933	3951	4748	80
H(25A)	−5938	5539	2917	80
H(25B)	−4396	4913	2297	80
H(25C)	−5806	3767	2871	80

[a] U_{eq} is defined as one third of the trace of the orthogonalized U_{ij} tensor.

Table 2. Anisotropic displacement parameters ($pm^2 \times 10^{-1}$). The anisotropic displacement factor has the following form: $-2\pi^2[(ha^*)^2U_{11} + ... + 2hka^*b^*U_{12}]$

	U11	U22	U33	U23	U13	U12
N(1)	30(2)	42(2)	46(2)	−19(2)	6(2)	−14(2)
O(1)	35(2)	59(2)	115(3)	−21(2)	8(2)	−8(2)
O(2)	39(2)	40(2)	80(2)	−20(2)	3(2)	−4(2)
O(3)	65(2)	66(2)	95(2)	−42(2)	42(2)	−11(2)
O(4)	47(2)	50(2)	63(2)	−12(2)	17(2)	−15(2)
O(5)	78(2)	78(2)	52(2)	−24(2)	−13(2)	4(2)
C(1)	30(2)	42(29	49(3)	−20(2)	7(2)	−12(2)
C(2)	27(2)	42(2)	38(2)	−15(2)	3(2)	−6(2)
C(3)	30(2)	35(2)	39(2)	−12(2)	−1(2)	−5(2)
C(4)	26(2)	38(2)	43(2)	−15(2)	5(2)	−8(2)
C(5)	31(2)	46(3)	46(2)	−21(2)	1(2)	−4(2)
C(6)	46(3)	53(3)	49(3)	−26(2)	13(2)	−19(2)
C(7)	35(2)	37(2)	55(3)	−17(2)	1(2)	−12(2)
C(8)	64(3)	53(3)	76(3)	−26(3)	−17(3)	−1(2)
C(9)	95(4)	77(4)	77(4)	−18(3)	−40(3)	−11(3)
C(10)	108(59)	87(4)	70(4)	−39(3)	−3(3)	−27(4)
C(11)	70(4)	73(4)	86(4)	−38(3)	8(3)	−10(3)
C(12)	49(3)	59(3)	58(3)	−24(2)	−5(2)	−9(2)
C(13)	30(2)	40(3)	49(3)	−15(2)	8(2)	−9(2)
C(14)	56(3)	44(3)	54(3)	−19(2)	−3(2)	−2(2)
C(15)	71(3)	47(3)	53(3)	−15(2)	−10(3)	1(2)
C(16)	44(3)	74(3)	37(3)	−15(3)	−2(2)	−5(3)
C(17)	52(3)	53(3)	54(3)	−21(2)	−7(2)	−4(2)
C(18)	47(3)	52(3)	45(3)	−17(2)	−6(2)	−2(2)
C(19)	109(4)	84(4)	57(3)	−27(3)	−24(3)	7(3)
C(20)	38(3)	54(3)	45(3)	−17(2)	1(2)	−11(2)
C(21)	49(3)	91(4)	66(3)	−5(3)	27(3)	−9(3)
C(22)	66(4)	312(9)	87(5)	55(5)	14(4)	13(5)
C(23)	44(3)	50(3)	36(2)	−12(2)	5(2)	−8(2)
C(24)	61(3)	52(3)	109(4)	−30(3)	3(3)	4(3)
C(25)	89(4)	70(4)	128(5)	−19(3)	−28(4)	10(3)

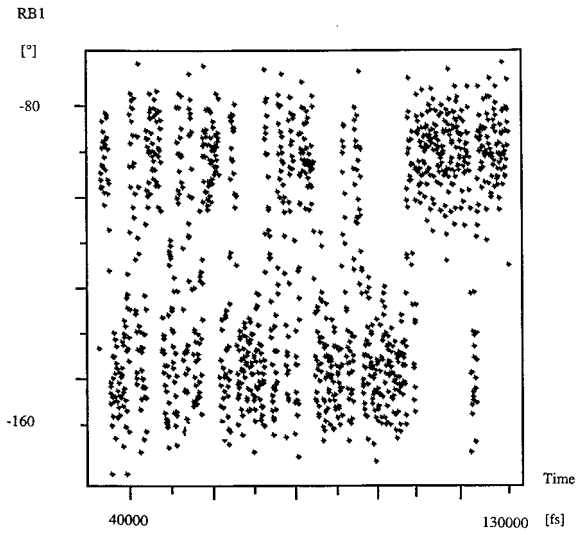

Figure 6. Torsion angle RB1 as function of time for conformer **2b**.

structure of **1** was observed, regarding the plane angles of the aromatic rings.

The chosen conformers **2a**–**c** were compared with the conformation of the azacyclic urea A-98881 in the complex with HIV-1 protease [19]. The aromatic residues of the latter show exact conformity in their location in the enzyme with those of cyclic urea **3** [19] as shown in Figure 3.

For the comparison the centroids of the aromatic residues of common methoxyphenyl and benzyl substituents of A-98881 and the three conformers of **2** were fitted. The best overlay was obtained for the energetically favourable conformation **2a**, where the centroids of the aromatic residues showed a nearly perfect match and also the angles between the ring planes were small (6.3°, 22°, 13.6°, 22.8°).

A CoMFA field fit with A-98881 as template was performed to align the molecules. The CoMFA field fit routine performs rigid body translation and rotation of the target molecule to optimize the degree of similarity of its steric and electrostatic fields with the template. After the field fit the energetically most favourable conformer **2a** showed a very good fit of the aromatic residues (rms 0.784) as shown in Figure 4 with a decrease of their plane angles to 5.6°, 8.3°, 13.4°, 7.7°.

The electrostatic potential (EP) of A-98881 and conformer **2a** displayed on the molecular surface show high similarity in the aromatic and hydroxymethylene group regions. In case of A-98881 the carbonyl urea possesses a more pronounced and directed negative potential than the corresponding hydroxymethylene group region of the cage dimer which might enable

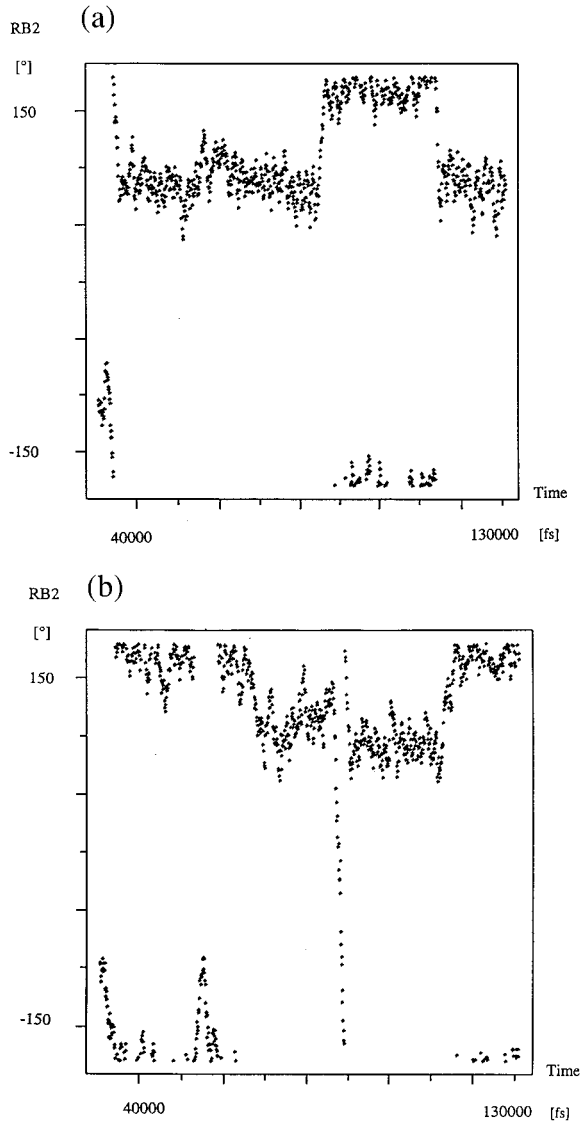

Figure 7. (a) Vacuum and (b) DMSO torsion angle RB2 as function of time for conformer **2c**. Negative values correspond to centrosymmetry, while positive values correspond to C_2-symmetry.

the molecule to a better hydrogen bonding to Ile 50 and Ile 50′ as will be discussed below (Figure 5a and b).

In order to investigate the flexibility of the aromatic residues of **2** which adopt in the conformers **2b** and **2c** twisted positions compared to A-98881 as well as to the cyclic urea **3**, a molecular dynamics simulation was performed with those conformers at 300 K. During the simulation the phenyl ring of the *N*-benzyl substituents rotated by 360°, but the rotatability

Table 3. Energy and important torsion angles of conformers **2a–c** and **2a(AM1)–2c(AM1)**

Conformation	Energy [kcal/mol]	RB1/RB1′ [°]	RB2/RB2′ [°]	RB3/RB3′ [°]
2a	74.98	−87.8/−88.1	103.1/104.5	72.5/75.1
2b	74.99	−136.3/−143.4	111.3/111.9	−75.7/−73.1
2c	79.97	−88.1/85.9	154.1/−148.4	165.8/−170.6
2a (AM1)	−89.13	−85.0/−82.5	113.8/110.2	67.9/85.1
2b (AM1)	−85.61	−152.0/−82.6	111.8/150.0	−11.0/−68.1
2c (AM1)	−85.34	−81.9/81.0	149.0/−147.8	168.8/−169.0

of the 4′-methoxyphenyl substituents was found to be limited, as they did not flip.

This result correlates well with measured ^{1}H-NMR data for the aromatic protons of the 4′-methoxyphenyl substituent, which show different signals for 2′-H and 6′-H at 7.67 and 7.20 ppm as well as for 3′-H and 5′-H at 6.69 and 6.49 ppm, respectively, according to their different magnetic environment due to the hindered rotation of the ring. However, the 4′-methoxyphenyl rings may adopt the orientation of the 3′-methoxyphenyl residue of A-98881 at room temperature. Both at 300 and 370 K the centrosymmetric conformer **2c** flipped to C_2-symmetry and remained in this conformation for most of the simulation time (Figure 7a). At 370 K the averaged structure of **2c** showed nearly perfect C_2-symmetry. As suggested by a referee also a simulation with DMSO as solvent was performed leading to identical results (Figure 7b).

Finally, a comparison of the binding properties of conformer **2a** with those of A-98881 in the enzyme was performed by calculating molecular interaction fields with certain probes using GRID. The chosen probes, CH_3 for alkyl, NHamide and carbonyl, O^- of COO^-, correspond to the functional groups of the active site cavity of the enzyme with which interactions may be possible. However, only conformer **2a** was considered, as both other conformers **2b** and **2c** can easily be converted to **2a** at room temperature as is evident from the molecular dynamics simulations.

For the CH_3 probe, corresponding to alkyl, at a contour level of −1.2 kcal/mol both fitted structures showed several regions for preferred interactions. Most favourable interactions were found for both compounds with the side chain of Ile 84′ and the Cα-atom of Gly 49′. From the contour maps A-98881 seemed to show more favourable interactions with Ile 50′ and Ala 28′ than conformer **2a** where only slight interactions to both Ile 50 and Ile 50′ and Ala 28′ are observed (Figure 8).

Certain conformities have been found for the second and third probe, NHamide and O^- of COO^-. The strongest interaction regions for the NHamide probe corresponded to the location of the calculated interaction minimas of A-98881 which are found near Ile 50 and Ala 28. Slight contacts appear to Ile 50′. A similar situation concerning Ile 50 as well as Ile 50′ can be stated for conformer **2a**. The location of the most favourable O^- interaction sites suggests marked contacts to Asp 25 for both structures (Figure 8).

The latter results correspond well to decisive binding properties of A-98881 derived from the X-ray crystal structure of the enzyme-inhibitor complex with hydrogen bonding of the hydroxy group to Asp 25/25′ and to the amide groups of Ile 50/50′ from the urea carbonyl group.

Conclusions

The centrosymmetical cage dimeric *N*-benzyl-3,5-bis(hydroxymethyl)-4-(4-methoxyphenyl)-1,4-dihydropyridine derived from X-ray crystal data of the corresponding 3,5-diethoxycarbonyl derivative has been investigated by molecular modeling as potential HIV-1 protease inhibitor and compared with the known inhibitor azacyclic urea A-98881. An energetically favourable conformer with C_2-symmetry showed an excellent fit with common aromatic residues of A-98881 and also some conformity of the electrostatic potential. In addition the regions of favourable interactions suggest similar binding properties for both structures to Asp 25/25′ as well as to Ile 50/50′ in the active site cavity of the enzyme. These results correlate well with first preliminary inhibition results

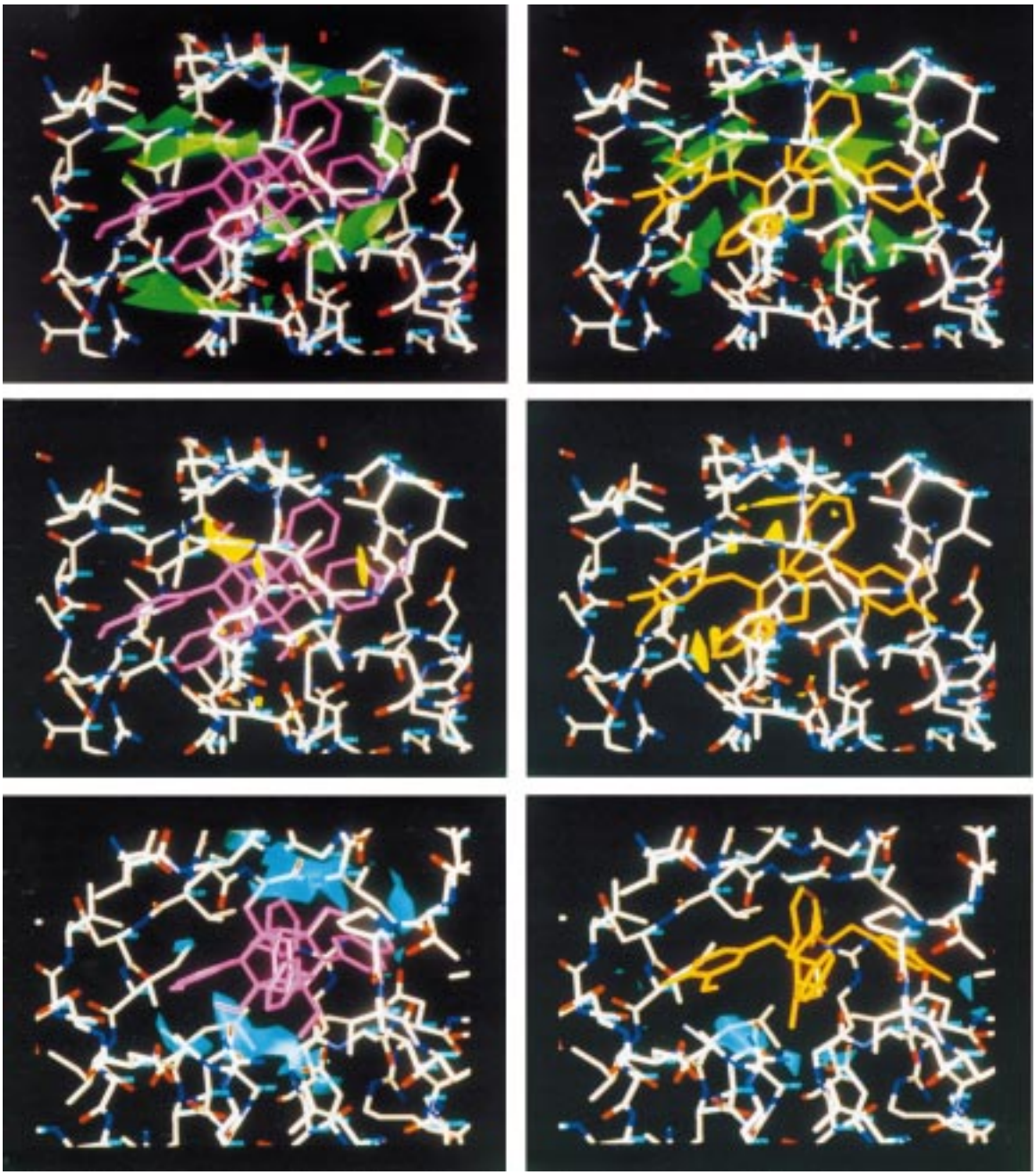

Figure 8. Most favourable interaction regions for the GRID probes CH_3 (green, −1.2 kcal/mol), NHamide (yellow, −5.0 kcal/mol) and O^- of COO^- (cyan, −4.0 kcal/mol) of conformer **2a** (left) and A-98881 (right). For a better viewing of the interaction regions for the latter GRID probe conformer **2a** (left) and A-98881 (right) are shown from a different point of view.

of this compound against HIV-1 protease [Hilgeroth, A., unpublished results]. Therefore cage dimeric 1,4-dihydropyridines could become a novel class of HIV-1 protease inhibitors.

Acknowledgements

Andreas Hilgeroth is grateful for the support of the work by the German Pharmaceutical Society (DPhG).

References

1. a. Gallo, R. C., Sarin, P. S., Gelman, E. P., Robert-Guroff, M., Richardson, E., Kalyanaraman, V. S., Mann, D., Sidhu, G. D., Stahl, R. E., Zolla-Prazner, S., Leibowitch, J. and Popovic, M., Science, 220 (1983) 865.
   b. Barre-Sinoussi, F., Cherman, J. C., Rey, F., Nugeyre, M. T., Chamaret, S., Gruest, J., Dauguet, C., Axler-Blin, C., Vezinet-Brun, F., Rouzioux, C., Rozenbaum, W. and Montagnier, L., Science, 220 (1983) 868.
2. Von der Helm, K., Biol. Chem., 377 (1996) 765.
3. Hilgeroth, A., Pharm. Zeit, 27 (1998) 22.
4. Wlodawer, A., Miller, M., Jaskolski, M., Sathyanarayana, B. K., Baldwin, E., Weber, I. T., Clawson, L., Schneider, J. and Kent, S. B. H., Science, 245 (1989) 616.
5. Seelmeier, S., Schmidt, H., Turk, V. and von der Helm, K., Proc. Natl. Acad. Sci. USA, 85 (1988) 6612.
6. Thaisrivongs, S., Annu. Rep. Med. Chem., 29 (1994) 133.
7. Hodge, C. N., Aldrich, P. E., Bacheler, L. T., Chang, Ch., Eyermann, Ch. J., Garber, S., Grubb, M., Jackson, D. A., Prabharkar, K. J., Koranz, B., Lam, P. Y. S., Maurin, M. B., Meek, J. L., Otto, M. J., Rayner, M. M., Reid, C., Sharpe, Th. R., Shum, L., Winslow, D. L. and Erickson-Viitanen, S., Chem. Biol., 3 (1996) 301.
8. Sham, H. L., Zhao, Ch., Stewart, K. D., Betebenner, D. A., Lin, Sh., Park, Ch. H., Kong, X., Rosenbrook, W., Jr., Herrin, Th., Madigan, D., Vasavanonda, S., Lyons, N., Molla, A., Saldivar, A., Marsh, K. C., McDonald, E., Wideburg, N. E., Denissen, J. F., Robins, T., Kempf, D. J., Plattner, J. J. and Norbeck, D. W., J. Med. Chem., 39 (1996) 392.
9. Hilgeroth, A., Chem. Lett., (1997) 1269.
10. Hilgeroth, A., Baumeister, U. and Heinemann, F. W., Eur. J. Org. Chem., (1998) 1213.
11. SHELXTL 5.03 for Siemens Crystallographic Research Systems, Siemens Analytical X-ray Instr., Madison, WI, U.S.A., 1995.
12. SYBYL, Tripos Associates Inc., St. Louis, MO.
13. Gasteiger, J. and Marseli, M., Tetrahedron, 36 (1980) 3219.
14. Gasteiger, J. and Saller, H., Angew. Chem., 97 (1985) 699.
15. Maurhofer, E. and Höltje, H.-D.: First Workshop on Molecular Modeling, May 1987, Darmstadt, Germany.
16. SYBYL Molecular Spreadsheet Manual V. 6.3, 192.
17. Clark, M., Cramer III, R. D. and Van Opdenbosch, N., J. Comput. Chem., 10 (1989) 982.
18. a. Goodford, P. J., J. Med. Chem., 7 (1985) 849.
    b. Molecular Discovery Ltd., Elms Parade, Oxford, U.K.
19. X-ray data of A-98881 and cyclic urea **3** are available in the Brookhaven Protein Data Bank under the ID codes 1HVR and 1PRO, respectively.